

Study of the topography of silicon surface evolution under irradiation by a gallium ion beam

M.A. Smirnova, V.I. Bachurin*, M.E. Lebedev, L.A. Mazaletsky, D.E. Pukhov, A.B. Churilov, A.S. Rudy

Valiev Institute of Physics and Technology of Russian Academy of Sciences, Yaroslavl Branch, Yaroslavl, 150007, Russia



ARTICLE INFO

Keywords:

Development of topography
Sputtering
Gallium ions
Silicon
Ripples

ABSTRACT

The silicon surface was irradiated with 30 keV gallium ion beam at incidence angles from 0 to 50° and fluences from $6 \cdot 10^{16}$ to $5 \cdot 10^{18} \text{ cm}^{-2}$. Surface topography was investigated by scanning electron microscopy. It was found that one of four types of a relief can be formed on the silicon surface depending on the ion beam incidence angle and these fluences. Pattern formation starts with fluences of $\sim 2 \cdot 10^{17} \text{ cm}^{-2}$. The peculiarities of a relief evolution can be explained by the angular dependences of silicon sputtering with gallium ion beam and the possible existence of implanted gallium in the near-surface layer in the form of precipitates.

1. Introduction

Surface sputtering with focused ion beams (FIB), which is used for samples preparation for transmission electron microscopy (TEM) and integrated circuits failure analysis, is now becoming widely used for the formation of nanostructures on the surface of different materials [1–9]. Depending on the type of substrate, ion energy and kind of ions, it is possible to form a certain nanostructures on the surface. The advantages of the FIB technique compared to others (electron-beam and photo-lithography) are the high rate of pattern formation, the ability to process different materials (semiconductors, metals, dielectrics), the localization and selectivity of the etching process, which greatly simplifies the technological process of the surface nanostructuring. Ion beam irradiation can be carried out at different incidence angles and at different fluences. Nevertheless, despite these advantages, the formation of nanoscale structures by FIB can be associated with a number of problems. One of them is related with the formation of topographic inhomogeneities on the bottom and lateral faces of the sputtering crater. Formation of the relief can lead to a change of the sputtering rate [10] and the reproducibility of the experimental results, especially in the case of structures with a high aspect ratio [11]. At the moment, there are only few experimental works devoted to the formation of the surface topography (generally in the form of ripples) under sputtering of the most commonly used materials with a gallium FIB [12–16]. This paper represents the results of an experimental study of the topography formation on the Si surface irradiated with a Ga⁺ ion beam at different fluences and

the ions incidence angles.

2. Experimental

The irradiation experiments of Si (100) with a 30 keV Ga⁺ ion beam were carried out in a Quanta 3D 200i facility. It is a dual-beam FIB-SEM system equipped with a Ga⁺ liquid metal ion source (LMIS). A Si (100) wafers with a natural oxide layer were used as samples. Beams with a diameter of 4 μm, 300 nm and 85 nm were used at following irradiation parameters: ion beam overlap percentage of 95% (for ion beam with diameter of 4 μm) and 50% (300 and 85 nm), 0.1 μs dwell time and serpentine scan type. In all experiments the ion beam current was I = 5 nA, the scan area was $20 \times 20 \mu\text{m}^2$, and the current density was j = 1.25 mA cm⁻² ($7.8 \cdot 10^{15} \text{ cm}^{-2} \text{ s}^{-1}$). The experiments were carried out at room temperature.

A series of the samples were prepared for the study. The incidence angle of the ion beam Θ is defined with respect to the surface normal and varied from 0 to 50° with 5° increments. The ion fluence D varied from $6 \cdot 10^{16}$ to $5 \cdot 10^{18} \text{ cm}^{-2}$. These experiments allowed to identify the main trends in the formation of the surface topography at the certain angular and fluence ranges.

To illustrate the ripples profile the SEM images of the samples transverse sections were prepared.

The initial analysis of the surface topography was performed using the Quanta 3D 200i facility (in-situ). A more detailed analysis of all samples was carried out ex-situ using a scanning electron microscope

* Corresponding author.

E-mail address: vibachurin@mail.ru (V.I. Bachurin).

Supra 40. The energy of the electron beam amounted to 10 and 20 keV and angles of view were equal 0 and 60°. The necessity of using both methods of topography study is caused by the results presented in Ref. [17]. There it was shown that during atmospheric extraction of Si samples containing Ag atoms in the near-surface layer, which do not form chemical compounds with Si, Ag atoms are displaced onto the surface in the process of Si oxidation. Moreover, the Si surface remains smooth during in-situ measurements, and after removing the samples from the vacuum chamber for ex-situ measurements is covered by Ag droplets. Implanted Ga ions also don't form chemical compounds with Si, but they are present in the near-surface layer as a precipitate of a few nm in size [18,19]. A comparison of in-situ and ex-situ images of the Si surface after irradiation with a Ga^+ ions shown that extraction of the samples to the atmosphere doesn't change the surface topography. At the same time, the quality of images obtained on the Supra 40 is significantly better. Therefore, this article provides images obtained on this machine.

3. Results and discussion

As a result of this study, the peculiarities of the Si surface topography evolution under the Ga^+ ion beam irradiation of different diameters, different ions incidence angles and fluences were experimentally established.

Fig. 1 shows SEM images of the Si surface obtained at normal incidence of the ion beam, fluence of 10^{18} cm^{-2} at different degrees of focusing: (a) ion beam with a diameter of 85 nm, (b) ion beam with a diameter of 4 μm .

Both samples were produced under identical conditions, except the ion beam diameter. Similar studies were carried out at other incidence angles and fluences of the ion beam. The identity of the images of structures on the surface of silicon obtained by ion beams with 4 orders of local current density magnitude difference indicates that the pattern is not depending on the beam diameter or the local ion flux. Using an ion beam with 4 μm diameter and 95% overlap practically mimics a broad ion beam irradiation. Images obtained from the surface irradiated by an ion beam with a diameter of 4 μm will be presented further in the paper because the reproducibility of the results was higher when the sample was irradiated with this beam.

Fig. 2 shows the topography of the Si surface irradiated by Ga^+ ions at normal and 25° incidence angles of the ion beam. It was found that during sputtering of the sample material at incidence angles in the range from 0 to 20°, starting with a fluence of $2 \cdot 10^{17} \text{ cm}^{-2}$, a granular structure with a grain size $\sim 35 \text{ nm}$ is formed on the surface and practically doesn't change with further increase of the fluence (**Fig. 2a** and b).

A granular structure is observed in the case of 25° incidence angle up to fluence of $4 \cdot 10^{17} \text{ cm}^{-2}$. In addition, some separate surface swellings are present (**Fig. 2c**).

Such swellings can be a consequence of Ga precipitates reaching the surface under ion sputtering. When a fluence increase up to $2 \cdot 10^{18} \text{ cm}^{-2}$, the grains are growing, thereby a grid-like structure is formed on the Si surface (**Fig. 2d**).

The topography of the Si surface irradiated with Ga^+ ions at $\theta = 30^\circ$ with different magnifications (5000 and 50 000 respectively) are

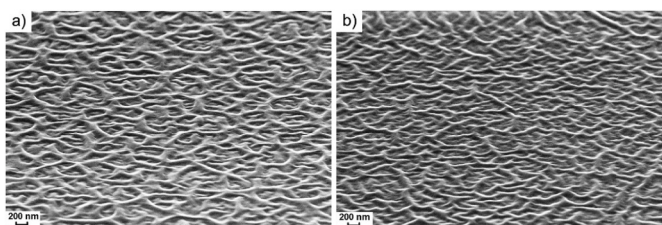


Fig. 1. SEM-images of Si surface after ion irradiation. Angle of incidence $\theta = 0^\circ$, ion fluence 10^{18} cm^{-2} . a) 85 nm, b) 4 μm ion beam diameter.

presented in **Fig. 3**.

The periodic ripples perpendicular to the plane of incidence of the primary beam are formed on the surface in this case.

Fig. 4 illustrates the sequential changes in the surface topography under fluences from $6 \cdot 10^{16} \text{ cm}^{-2}$ up to $4 \cdot 10^{18} \text{ cm}^{-2}$. One can see the appearance of the nanometric droplets on the surface at fluence $D = 6 \cdot 10^{16} \text{ cm}^{-2}$. The elemental maps obtained by energy dispersive X-ray microanalysis showed that these hills are gallium enriched. It was shown in Refs. [18,19] that implanted Ga in the near-surface layer exists in the form of precipitates $\sim 10 \text{ nm}$ in size, located at a depth of 10–20 nm. Apparently, at $D \sim 6 \cdot 10^{16} \text{ cm}^{-2}$, Ga precipitates appear onto the surface and merge into larger droplets (**Fig. 4a**). The difference between the Si and Ga sputtering rates leads to the formation of topographic inhomogeneities in the form of hills and troughs (**Fig. 4b**) which subsequently initiates the formation of a wave-like relief (**Fig. 4c**). Starting with a fluence of $2 \cdot 4 \cdot 10^{17} \text{ cm}^{-2}$ up to $2 \cdot 10^{18} \text{ cm}^{-2}$ one can see the formation of ripples (**Figs. 3 and 4c**). The intersection and merging of the waves are observed and starting from the fluence of $4 \cdot 10^{18} \text{ cm}^{-2}$ the ripples are destroyed keeping the periodicity pattern. In the considered range of fluences, the average value of the wavelength changes in the limits from 150 to 800 nm, and the amplitude from 30 to 70 nm (**Fig. 5**), which agrees well with the data obtained in Refs. [12,13].

In the case of Si irradiation by Ga^+ ions at angle of incidence of 35° (starting with a fluence $D = 2 \cdot 10^{17} \text{ cm}^{-2}$) hills appear on the surface and ripples perpendicular to the plane of incidence of the ion beam are observed. At the fluence $D = 2 \cdot 10^{18} \text{ cm}^{-2}$ two areas are distinguished on the irradiated surface of the sample, one of which contains the wave vector of a relief coinciding with the beam direction, while in the other one it is rotated by a certain angle (**Fig. 6c**). In Ref. [13], a rotation of a wave vector of the wavelike relief with increasing fluence is reported, the reasons of which are not clear.

Fig. 7 illustrates the topography of the Si surface irradiated by Ga^+ ions at the incidence angles of the ion beam 40° (a) and 45° (b). In the case of the ion beam incidence at an angle of 40°, there are non-contrast and non-periodic irregularities on the surface, which are smoothed by further increasing the fluence. And at an incidence angles of $\theta > 45^\circ$, the irradiated surface remains smooth over the studied range of the fluences.

Table 1 summarizes the main irradiation parameters and the types of inhomogeneities that arise from them.

An important feature of all types of relief observed on the silicon surface at ion beam incidence angles less than 40° is that the formation of structures occurs at fluences slightly higher than the fluence corresponding to the start of the erosion process. It was shown in Refs. [18, 20] erosion of surface of Si by a 30 keV Ga^+ ion beam becomes appreciable starting with the fluence $D \sim 3 \cdot 10^{16} \text{ cm}^{-2}$ and at a fluence of $6 \cdot 10^{16} \text{ cm}^{-2}$ the sputtering crater depth amounts to $\sim 10 \text{ nm}$. As noted above, it was experimentally established in Refs. [18,19] that Ga atoms in the near-surface layer of Si exist in the form of precipitates dissolved in this layer a few nm in size, located in two layers at a depth of 10–20 nm (Si was irradiated at normal ion beam incidence with a fluence of 10^{17} cm^{-2}). This means that relief nucleation at incidence angles close to the surface normal starts at the depths corresponding to the Ga precipitate depth location in the near-surface layer of Si. The surface binding energy of Ga atoms is almost two times less than that of the Si atoms. The difference in the sputtering yields [21] of Ga and Si in the surface layer provides the development of the observed topographic inhomogeneities.

Differences in the shape of the topography of the Si surface irradiated with Ga^+ ions at different incidence angles are apparently related to the different content of implanted gallium near the surface. A recent study [22] determined the angular dependences of the surface layer composition and the sputtering yields due to the bombardment of the Si surface with 30 keV Ga^+ ions. **Fig. 8** shows the angular dependences of Ga content near the surface, obtained by integration of Ga concentration profiles measured by SIMS analysis and on the surface measured by the AES. It can be noticed that the concentration of Ga in the near-surface layer ($\sim 30 \text{ nm}$) is about 30% at incidence angles from 0 to 20°. At the

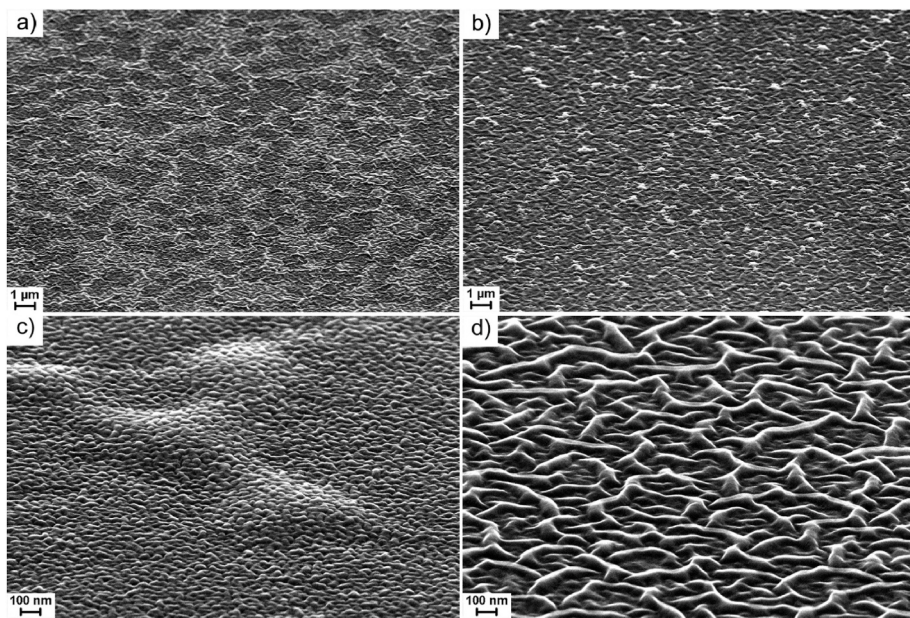


Fig. 2. SEM-images of Si surface after ion irradiation. Angles of incidence: $\theta = 0^\circ$ (a, b), 25° (c, d), ion fluences: $2 \cdot 10^{17}$ (left column), $2 \cdot 10^{18} \text{ cm}^{-2}$ (right column).

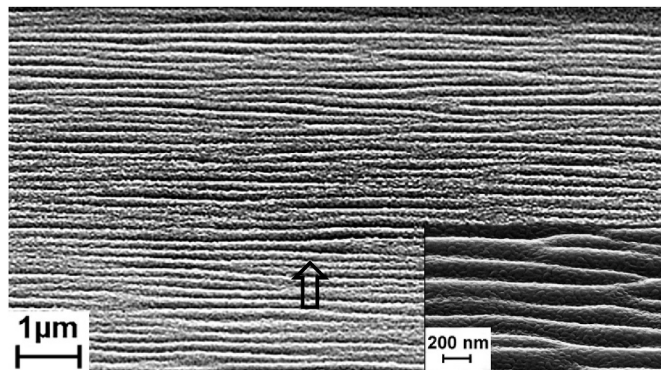


Fig. 3. Micrographs of ripples on the Si surface. Angle of incidence $\theta = 30^\circ$. Ion fluence 10^{18} cm^{-2} . The arrow indicates the direction of incidence of the ion beam.

same time, it reaches 60% on the surface. With increasing an angle of incidence, the Ga content in the layer and on the surface decreases rather sharply and it is less than 10–15% at $\Theta > 40^\circ$. Apparently, the low Ga concentration in the near-surface layer at these incidence angles is the reason of absence of noticeable relief on the surface at fluences up to $5 \cdot 10^{18} \text{ cm}^{-2}$.

The peculiarity of the appearance of ripples on the Si surface under irradiation with 30 keV Ga^+ is that it occurs at sufficiently low ion fluences ($D = 4 \cdot 10^{17} \text{ cm}^{-2}$) or at small depths of sputtering craters ($\sim 150 \text{ nm}$). It's known that ripples appear on the Si surface under irradiation with 20 keV Ar^+ ions at a sputtering crater depth of $\sim 44 \mu\text{m}$ (critical fluence $D = 6 \cdot 10^{19} \text{ cm}^{-2}$) [23]; with 12.5 keV O_2^+ ions $\sim 1 \mu\text{m}$ [24]; with 9 keV N_2^+ ions $\sim 0.2 \mu\text{m}$ [25]. So, the critical fluences for ripples nucleation during bombardment with ions of inert and chemically active gases differ by 1–2 orders of magnitude. Such differences can be explained by the existence of silicon oxide and silicon nitride precipitates [26–28] in the near-surface layer during oblique incidence of ion beams. Heterogeneity of the near-surface layer leads to the formation of an arbitrary initial relief on the surface due to the difference in sputtering rates of silicon and its compounds. This initial relief initiates the generation of ripples. Under bombardment by ions of inert gases, the accumulated bulk defects can initiate the appearance of a wave-like

relief, which determines the high fluences that precede the appearance of ripples [23].

One of the first models explaining the formation of ripples [29] combines the effects of sputtering and surface diffusion and is based on the sputtering theory of Sigmund [30]. It relates the rate of atom removal to the energy deposited by incident ion into surface layer. The coefficients in proposed equation [29] are functions of the ion beam parameters and relate the sputtering yield at any point on the surface to the local curvature. Thus, the presence of the original surface local curvature is necessary. Later in the work [31] it is stated, that transition between the flat and rippled states of the surface is not possible. To explain the appearance of the initial surface topography leading to a change of the local angle of ion incidence the term $\eta(x,y,t)$ which accounts the stochastic nature of the current density of incident ions was introduced in the equation of a nonlinear model of ripple formation [32]. From a practical point of view, accounting of this summand seems to be quite difficult. Therefore, in Ref. [33] it was suggested to substitute it for an arbitrary initial relief in the modeling of the formation of the wave-like relief. This approach led the authors to the results of modeling structures that quite well consistent with the experimental results.

The effect of topographic inhomogeneities on the ripple nucleation process was demonstrated experimentally in Refs. [34,35]. As was shown in Ref. [34], the presence of Au islands on the Si surface leads to almost immediate formation of ripples on the Si surface under N_2^+ ion bombardment with the same wavelength as under irradiation of pure Si surface after reaching the critical fluence of ripple nucleation. In Ref. [35] it was shown that the initial surface roughness on the Si surface which was formed by a preliminary chemical treatment with 16.7 keV O_2^+ ions leads to a two orders of magnitude reduction of the ion fluence required for a relief nucleation on the Si surface under 16.7 keV O_2^+ ion bombardment. Recently, a fairly large number of works have appeared that consider processes of relief formation on the surface of various materials, including Si, during simultaneous sputtering by inert gas ions and deposition of metal atoms [17,36–38] and bombardment by metal ions [35]. According to the opinion of the authors [17,37,39], the existence of metal silicides in the near-surface layer is one of the necessary conditions for the ripples formation. The higher sputtering rate of Si compared to silicides of metals leads to the appearance of topographic inhomogeneities on the surface, initiating the appearance of a periodic relief. Therefore, it is possible to conclude that the existence of Ga precipitates in the near-surface layer of Si, which rate exceeds the

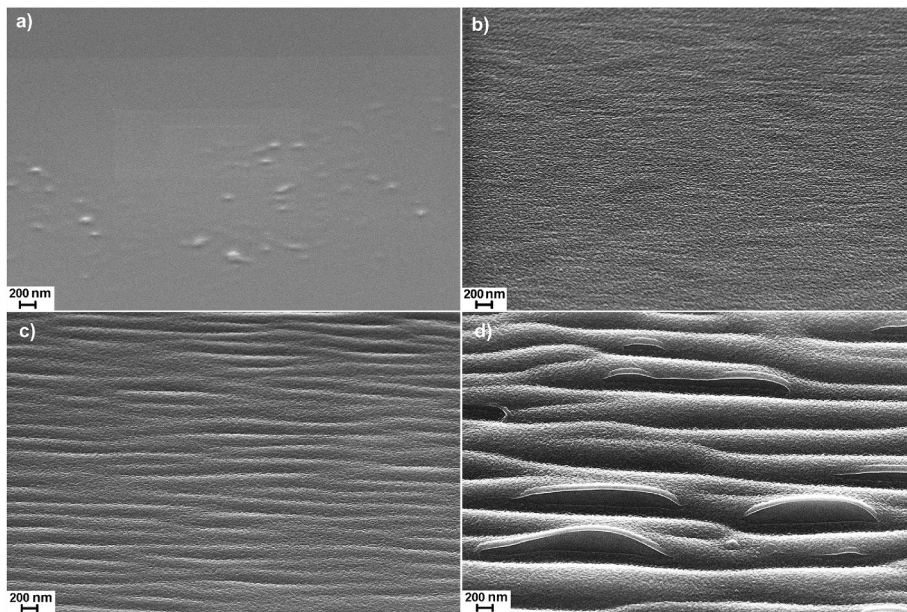


Fig. 4. SEM images of the Si surface irradiated by Ga ion beam. Angle of incidence $\theta = 30^\circ$. Ion fluences: a) $6 \cdot 10^{16}$, b) $2 \cdot 10^{17}$, c) $8 \cdot 10^{17}$, d) $4 \cdot 10^{18} \text{ cm}^{-2}$.

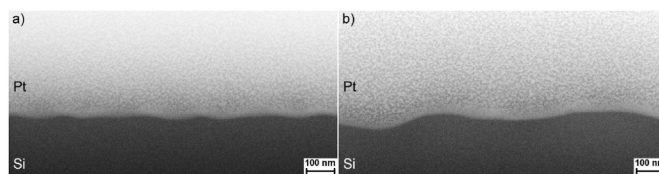


Fig. 5. SEM images of the cross section of the Si surface irradiated with a Ga^+ ion beam at an angle of 30° with irradiation doses of: (a) $4 \cdot 10^{17}$ and (b) $2 \cdot 10^{18} \text{ cm}^{-2}$.

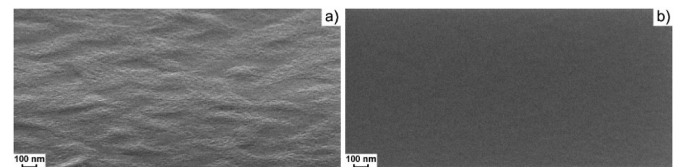


Fig. 7. Micrographs of the Si surface after ion irradiation. Ion fluence $D = 10^{18} \text{ cm}^{-2}$. Angles of incidence: a) 40° , b) 45° .

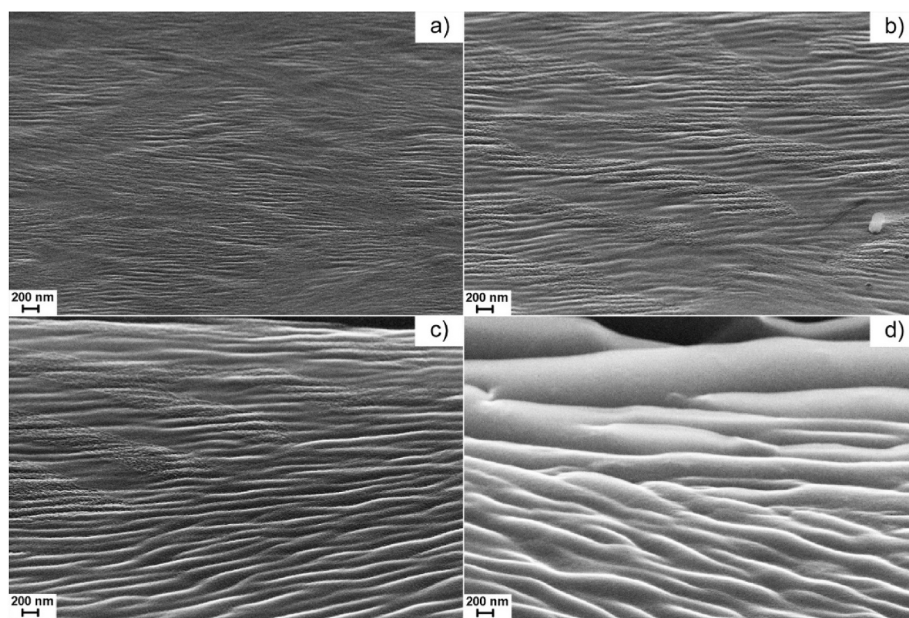


Fig. 6. Micrograph of a ripple structures on the Si surface after ion irradiation. Angle of incidence $\theta = 35^\circ$. Ion fluences: a) $2 \cdot 10^{17}$, b) $4 \cdot 10^{17}$, c) $2 \cdot 10^{18}$, d) $4 \cdot 10^{18} \text{ cm}^{-2}$.

Table 1
Summary of experimental data.

θ , grad	D, cm^{-2}	Type of a relief
0–20	$2 \cdot 10^{17} - 4 \cdot 10^{18}$	a granular structure
25	$4 \cdot 10^{17} - 4 \cdot 10^{18}$	a grid-like structure
30–35	$4 \cdot 10^{17} - 4 \cdot 10^{18}$	a periodic ripple relief
40	$4 \cdot 10^{17} - 4 \cdot 10^{18}$	a non-periodic irregularities
45–50	$6 \cdot 10^{16} - 4 \cdot 10^{18}$	a smooth surface

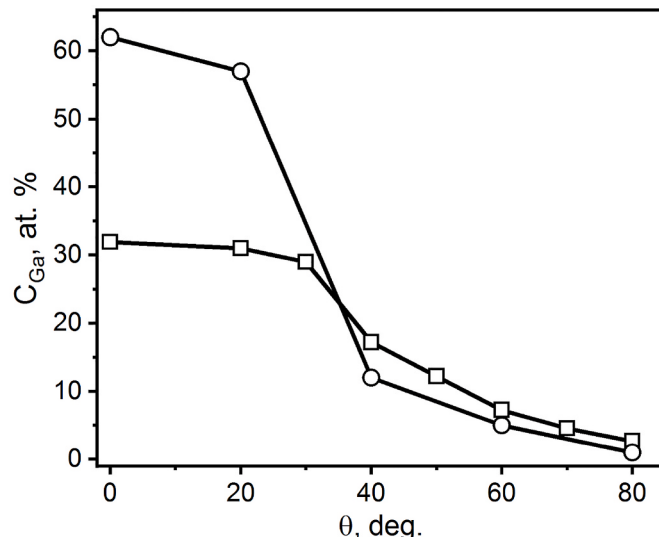


Fig. 8. Angular dependences of Ga concentration in Si surface layer based on SIMS (square tags) and AES (circle tags) data [22].

sputtering rate of the surrounding silicon, leads to the formation of topographic inhomogeneities and the rapid appearance of ripples.

4. Conclusions

The process of the Si (100) surface topography evolution under irradiation with a 30 keV Ga⁺ ion beam with fluences D = $6 \cdot 10^{16} - 5 \cdot 10^{18} \text{ cm}^{-2}$ at incidence angles of θ from 0 to 50° was studied. Irradiation of Si with Ga ions was carried out on the Quanta 3D 200i dual beam microscope. The surface topography was analyzed with SEM by using the Quanta 3D 200i (in situ) and the Supra 40 (ex situ) facilities.

According to the experimental results, it can be concluded that four types of inhomogeneities can be observed on the Si surface under sequentially changing the ion beam incidence angle from 0 to 50° in the studied range of fluences: a granular structure, a grid-like structure, a periodic wave-like structure and a non-periodic irregularities.

The peculiarity of all relief types at ion beam incidence angles less than 40° is that the formation of structures occurs at fluences slightly higher than the fluence needed for the high rate of formation. The reason for the early development of topographic inhomogeneities is that the implanted Ga is located in the form of precipitates lying at a depth of 10–20 nm at ion beam incidence angles close to the surface normal. By increasing the ion beam incidence angle, the concentration of implanted Ga in the near-surface layer of Si significantly decreases but remains observable up to 40°. The possible existence of Ga in the form of precipitates near the surface leads to the rapid development of a relief of the irradiated surface due to the difference in sputtering yields of Si and Ga.

The results obtained by studying of the Si surface topography under Ga ion beam irradiation allow proposing usage of the gallium FIB for formation of microstructures on the Si surface at incidence angles of ion beam exceeding $\theta = 45^\circ$. This helps to improve the reproducibility of the results of surface structuring.

CRediT authorship contribution statement

M.A. Smirnova: Investigation. **V.I. Bachurin:** Conceptualization. **M.E. Lebedev:** Investigation. **D.E. Pukhov:** Investigation. **A.B. Churilov:** Investigation. **A.S. Rudy:** Supervision.

Declaration of competing interest

The authors declare that they have no known competing financial interests or personal relationships that could have appeared to influence the work reported in this paper.

Acknowledgments

This study was performed with financial support from the Ministry of Education and Science of the Russian Federation within the framework of the state assignment of the Yaroslavl Branch of the Valiev Institute of Physics and Technology of Russian Academy of Sciences of topic № FFNN-2022-0018 and using equipment of the Facilities Sharing Center of scientific equipment “Diagnostics of micro and nanostructures”.

References

- [1] A. Sharma, B.N. Suma, K.N. Bhat, A.K. Naik, Gallium-doped piezoresistive sensor with optimized focused ion beam implantation, *J. Micromech. Syst.* 26 (2017) 127–134, <https://doi.org/10.1109/JMEMS.2016.2620801>.
- [2] Y. Fu, N.K.A. Bryan, Fabrication of three-dimensional microstructures by two-dimensional slice by slice approaching via focused ion beam milling, *J. Vac. Sci. Technol., B* 22 (4) (2004) 1672–1678, <https://doi.org/10.1116/1.1761460>.
- [3] Y. Zhang, G. Ran, Self-assembly of well-ordered and highly uniform nanoripples induced by focused ion beam, *Phys. E Low-dimens. Syst. Nanostruct.* 41 (2009) 1848–1852, <https://doi.org/10.1016/j.physe.2009.08.001>.
- [4] N. Yao, A. Epstein, Surface nanofabrication using focused ion beam, *Microscopy Book Series*, in: A. Méndez-Vilas, J. Diaz (Eds.), *Microscopy: Science, Technology, Applications and Education* vol. 3, 2010, pp. 2190–2199, №4.
- [5] M.Y. Ali, W. Hung, F. Yongqi, A review of focused ion beam sputtering, *Int. J. Precis. Eng. Manuf.* 11 (2010) 157–170, <https://doi.org/10.1007/s12541-010-0019-y>.
- [6] X. Xu, J. Wu, X. Wang, H. Li, Z. Zhou, Z.M. Wang, Site-controlled fabrication of Ga nanodroplets by focused ion beam, *Appl. Phys. Lett.* 104 (2014), 133104, <https://doi.org/10.1063/1.4870421>.
- [7] A. Joshi-Imre, S. Bauerdiick, Direct-write ion beam lithography, *J. of Nanotechnology* (2014) 1–26, <https://doi.org/10.1155/2014/170415>.
- [8] X. Xu, J. Wu, X. Wang, M. Zhang, J. Li, Z. Shi, H. Li, Z. Zhou, H. Ji, X. Niu, Z. M. Wang, Ion-beam-directed self-ordering of Ga nanodroplets on GaAs surfaces, *Nanoscale Res. Lett.* 11 (2016) 11–38, <https://doi.org/10.1186/s11671-016-1234-y>.
- [9] L. Bruchhaus, P. Mazarov, L. Bischoff, J. Gierak, A.D. Wieck, H. Hovel, Comparison of technologies for nano device prototyping with a special focus on ion beams: a review, *Appl. Phys. Rev.* 4 (2017), 011302, <https://doi.org/10.1063/1.4972262>.
- [10] G. Carter, The effects of surface ripples on sputtering erosion and secondary ion emission yields, *J. Appl. Phys.* 85 (1999) 455–459, <https://doi.org/10.1063/1.369408>.
- [11] W. MoberlyChan, Surface modification energized by FIB: the influence of etch rates & aspect ratio on ripple wavelengths, *MRS Symp. Proc.* 960 (2006), <https://doi.org/10.1557/PROC-0960-N10-02-LL06-02>.
- [12] S. Habenicht, K.P. Lieb, J. Koch, A.D. Wieck, Ripple propagation and velocity dispersion on ion-beam-eroded silicon surfaces, *Phys. Rev. B* 65 (2002), 115327, <https://doi.org/10.1103/PhysRevB.65.115327>.
- [13] H.X. Qian, W. Znou, Ripple rotation on ion sputtered Si (100), *Mater. Lett.* 77 (2012) 113–116, <https://doi.org/10.1016/j.matlet.2012.03.003>.
- [14] H. Gnaser, B. Reuscher, A. Zeuner, Propagation of nanoscale ripples on ion-irradiated surfaces, *Nucl. Instrum. Methods B* 285 (2012) 142–147, <https://doi.org/10.1016/j.nimb.2012.05.028>.
- [15] F. Datta, Yuh-Renn Wu, Y.L. Wang, Real-time observation of ripple structure formation on a diamond surface under focused ion-beam bombardment, *Phys. Rev. D* 63 (2001), 125407, <https://doi.org/10.1103/PhysRevD.63.125407>.
- [16] D.P. Adams, M.J. Vasile, T.M. Mayer, V.C. Hodges, Focused ion beam milling of diamond: effects of H₂O on yield, surface morphology and microstructure, *J. Vac. Sci. Technol., B* 21 (2003) 2334–2343, <https://doi.org/10.1116/1.1619421>.
- [17] M. Engler, F. Frost, S. Muller, S. Masko, M. Will, R. Feder, D. Spemann, R. Hubner, S. Fasko, T. Michely, Silicide induced ion beam patterning of Si(001), *Nanotechnology* 25 (2014), 115303, <https://doi.org/10.1088/0957-4484/25/11/115303>.
- [18] L. Frey, C. Lehrer, H. Ryssel, Nanoscale effects in focused ion beam processing, *Appl. Phys. A* 76 (2003) 1017–1023, <https://doi.org/10.1007/s00339-002-1943-1>.
- [19] M. Rommel, G. Spoldi, V. Yanev, S. Beuer, B. Amon, J. Jambreck, S. Petersen, A. J. Bauer, Comprehensive study of focused ion beam induced lateral damage in

- silicon by scanning probe microscopy techniques, *J. Vac. Sci. Technol., B* 28 (2010) 595–607, <https://doi.org/10.1116/1.3431085>.
- [20] C. Lehrer, L. Frey, S. Petersen, H. Ryssel, Limitations of focused ion beam nanomachining, *J. Vac. Sci. Technol., B* 19 (2001) 2533, <https://doi.org/10.1116/1.1417553>.
- [21] Sputtering by particle bombardment II, in: R. Behrisch (Ed.), *Topics Appl. Phys.*, vol. 52, Springer, Berlin, Heidelberg, New York, 1981, <https://doi.org/10.1007/3-540-12593-0>.
- [22] V.I. Bachurin, I.V. Zhuravlev, D.E. Pukhov, A.S. Rudy, S.G. Simakin, M. A. Smirnova, A.B. Churilov, *J. Surf. Invest.: X-Ray, Synchrotron Neutron Tech.* 14 (2020) 784–790, <https://doi.org/10.1134/S1027451020040229>.
- [23] G. Carter, V. Vishnyakov, Ne^+ and Ar^+ ion bombardment-induced topography on Si, *Surf. Interface Anal.* 23 (1995) 514–520, <https://doi.org/10.1002/sia.740230711>.
- [24] K. Elst, W. Vandervorst, Influence of the composition of the altered layer on the ripple formation, *J. Vac. Sci. Technol., A* 12 (1994) 3205–3216, <https://doi.org/10.1116/1.579239>.
- [25] V.K. Smirnov, D.S. Kibalov, S.A. Krivelevich, P.A. Lepshin, E.V. Potapov, R. A. Yankov, W. Skorupa, V.V. Makarov, A.B. Danilin, Wave-ordered structures formed on SOI wafers by reactive ion beams, *Nucl. Instrum. Methods B* 147 (1999) 310–315, [https://doi.org/10.1016/S0168-583X\(98\)00610-7](https://doi.org/10.1016/S0168-583X(98)00610-7).
- [26] K. Wittmaack, Local SiO_2 formation in silicon bombarded with oxygen above the critical angle for beam-induced oxidation: new evidence from sputtering yield ratios and correlation with data obtained by other techniques, *Surf. Interface Anal.* 29 (2000) 721–725, [https://doi.org/10.1002/1096-9918\(200010\)29:10%3C721::AID-SIA916%3E3.0.CO;2-Q](https://doi.org/10.1002/1096-9918(200010)29:10%3C721::AID-SIA916%3E3.0.CO;2-Q).
- [27] S. Bhattacharjee, P. Karmakar, A. Chakrabarti, Key factors of ion induced nanopatterning, *Nucl. Instrum. Methods B* 278 (2012) 58–62, <https://doi.org/10.1016/j.nimb.2012.02.004>.
- [28] V.I. Bachurin, P.A. Lepshin, V.K. Smirnov, Angular dependences of surface composition, sputtering and ripple formation on silicon under N_2^+ ion bombardment, *Vacuum* 56 (2000) 241–245, [https://doi.org/10.1016/S0042-207X\(99\)00194-3](https://doi.org/10.1016/S0042-207X(99)00194-3).
- [29] R.M. Bradley, M.E. Harper, Theory of ripple topography induced by ion bombardment, *J. Vac. Sci. Technol., A* 6 (1988) 2390–2395, <https://doi.org/10.1116/1.575561>.
- [30] P. Sigmund, A mechanism of surface micro-roughening by ion bombardment, *J. Mater. Sci.* 8 (1973) 1545.
- [31] P.D. Shipman, R.M. Bradley, Theory of nanoscale pattern formation induced by normal-incidence ion bombardment of binary compounds, *Phys. Rev. B* 84 (2011), 085420, <https://doi.org/10.1103/PhysRevB.84.085420>.
- [32] R. Cuerno, A.I. Barbasi, Dynamic scaling of ion-sputtered surfaces, *Phys. Rev. Lett.* 74 (1995) 4746–4749, <https://doi.org/10.1103/PhysRevLett.74.4746>.
- [33] B. Kahng, H. Jeong, A.I. Barbasi, Quantum dot and hole formation in sputter erosion, *Appl. Phys. Lett.* 78 (2001) 805–807, <https://doi.org/10.1063/1.1343468>.
- [34] V.K. Smirnov, D.S. Kibalov, P.A. Lepshin, V.I. Bachurin, Influence of topographical irregularities on on the process of formation of wave micro relief on silicon surfaces, *Izv. Akad. Nauk, Ser. Fiz.* 64 (2000) 626–630 (in Russian).
- [35] P. Karmakar, S.A. Mollick, D. Ghose, A. Chakrabarti, Role of initial surface roughness on ion induced surface morphology, *Appl. Phys. Lett.* 93 (2008), 103102, <https://doi.org/10.1063/1.2974086>.
- [36] S. Masko, F. Frost, B. Ziberi, D.F. Forster, T. Michely, Is keV ion-induced pattern formation on Si(001) caused by metal impurities? *Nanotechnology* 21 (2010), 085301 <https://doi.org/10.1088/0957-4448/21/8/085301>.
- [37] K. Zhang, O. Bobes, H. Hofsäss, Designing self-organized nanopatterns on Si by ion irradiation and metal co-deposition, *Nanotechnology* 25 (2014), 085301, <https://doi.org/10.1088/0957-4448/25/8/085301>.
- [38] Y. Liu, D. Hirsch, R. Fechner, Y. Hong, S. Fu, F. Frost, B. Rausdhebach, Nanostructures on fused silica surfaces produced by ion beam sputtering with Al co-deposition, *Appl. Phys. A* 124 (2018) 73–91, <https://doi.org/10.1007/s00339-017-1393-4>.
- [39] A. Redondo-Cubero, K. Lorenz, F.J. Palomares, A. Munoz, M. Catro, J. Munoz-Garcia, L. Vzquez, Concurrent segregation and erosion effects in medium-energy iron beam patterning of silicon surfaces, *J. Phys.: Condens. Mater.* 30 (2018), 274001, <https://doi.org/10.1088/1361-648X/aac79a>.